Citation: Molecular Therapy–Nucleic Acids (2013) 2, e73; doi:10.1038/mtna.2012.64

www.nature.com/mtna

METHODS: ORIGINAL ARTICLE

Focal Delivery of AAV2/1-transgenes Into the Rat Brain by Localized Ultrasound-induced BBB Opening

Angelika Alonso[1], Eileen Reinz[2], Barbara Leuchs[2], Jürgen Kleinschmidt[2], Marc Fatar[1], Bart Geers[3], Ine Lentacker[3], Michael G. Hennerici[1], Stefaan C. de Smedt[3] and Stephen Meairs[1]

Delivery of drugs and macromolecules to the central nervous system (CNS) is hindered by the blood–brain barrier (BBB). Several approaches have been used to overcome this hindrance to facilitate the treatment of various CNS diseases. We now present results showing that chimeric adeno-associated virus 2/1 (AAV2/1) particles containing the coding region for the *LacZ* gene are efficiently delivered into the rat brain upon intravenous (IV) administration after BBB opening by focused ultrasound in the presence of vascular acoustic resonators. We show that the transgene is correctly and efficiently expressed in cells located in the neighborhood of the insonated focus, especially in the vicinity of small vessels and capillaries. Histochemical LacZ staining allows the identification of large amounts of cells expressing the enzymatically active protein. Using double immunofluorescence (IF) with antibodies against tubulinIII and bacterial LacZ, we identified these cells to be mostly neurons. A small proportion of the transduced cells was recognized as glial cells, reacting positive in the IF with antibodies against astrocytic markers. These results demonstrate that our approach allows a very specific, localized, and efficient expression of intravenously administered transgenes in the brain of rats upon ultrasound-induced BBB opening.

Molecular Therapy–Nucleic Acids (2013) **2**, e73; doi:10.1038/mtna.2012.64 published online 19 February 2013
Subject Category: Methods

Introduction

Gene and drug delivery to the central nervous system (CNS) is delimitated through the blood–brain barrier (BBB).[1,2] Both the transcellular and paracellular pathway are strictly controlled by special cellular features, including a dense tight junctional network of the BBB endothelium and limited pinocytotic activity.[1,2] To facilitate drug delivery, several approaches to overcome the BBB have been investigated. Recently, it has been demonstrated that focused ultrasound in combination with ultrasound contrast agents (UCA) can lead to a transient disruption of the BBB without relevant neuronal damage.[3–6] As an underlying molecular mechanism of ultrasonographic BBB opening, both a transient disintegration of tight junctional complexes[7] and an increased caveolae-mediated transcellular transport have been discussed.[8] By this means, macromolecules such as antibodies[9] or plasmid DNA for nonviral gene therapy[10] have successfully been delivered in rodents.

Gene-targeted therapeutic approaches provide a new hope for several neurological diseases including a variety of neurodegenerative disorders. Recent and ongoing clinical trials investigate the therapeutic potential of gene delivery of neurotrophic factors in Parkinson's disease[11] and Alzheimer's disease[12] by intraparenchymal injection of adeno-associated viral vectors. Recombinant adeno-associated virus (rAAV) vectors have successfully been used for gene transfer to various regions of the CNS with favorable vector characteristics.[13,14] rAAV vectors proved to be nontoxic with low immune reaction compared with other viral vectors such as adenovirus.[15] Furthermore, a stable long-term gene expression[16] with high yield can be achieved. The cell tropism and regional transduction pattern of rAAV in the CNS depends on the serotype. Following direct injection into the CNS, the most commonly applied rAAV serotype 2 (rAAV2) has been shown to transduce mainly neurons, whereas rAAV4 transduction was only found in ependymal cells, and rAAV5 transduces both ependymal and neuronal cells.[17] Cross-packaging of AAV inverted terminal repeats into capsids of another serotype allows further modifications of the cellular tropism in the absence of differences in cis-acting elements.[18] Pseudotyped viruses with rAAV2 inverted terminal repeats showed highest transduction rates and widest distribution when packaged into capsids of AAV1 or AAV5 (rAAV2/1, rAAV2/5) compared with the nonchimeric rAAV 2/2.[19]

A broad clinical application in CNS diseases has been impeded so far as the intraparenchymal delivery using neurosurgically placed catheters is associated with a high rate of peri- and postinterventional complications.[11] Vascular delivery of rAAV to CNS neurons, however, has been ineffective so far as most AAV vectors do not cross the BBB. Recently, it has been shown that the AAV9 type may target neurons in rodents[20] after intravascular administration. However, a high peripheral tropism together with a limited neuronal transduction and pre-existing neutralizing antibodies in nonhuman

[1]Department of Neurology, Universitätsmedizin Mannheim, University of Heidelberg, Mannheim, Germany; [2]German Cancer Research Center, Heidelberg, Germany; [3]Laboratory of General Biochemistry & Physical Pharmacy, Ghent University, Gent, Belgium. Correspondence: Angelika Alonso, Department of Neurology, Universitätsmedizin Mannheim, University of Heidelberg, Theodor-Kutzer-Ufer 1–3, 68167, Mannheim, Germany. E-mail: alonso@neuro.ma.uni-heidelberg.de
Keywords: AAV; blood–brain barrier; ultrasound
Received 17 September 2012; accepted 13 December 2012; advance online publication 19 February 2013. doi:10.1038/mtna.2012.64

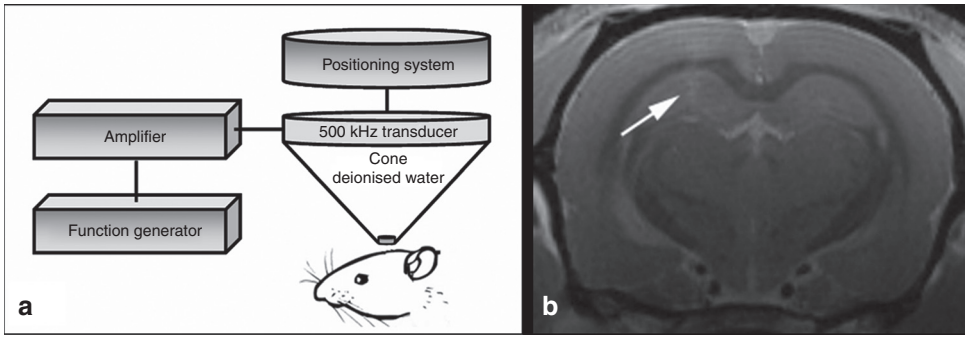

Figure 1 Experimental set-up and verification of BBB opening. (**a**) One hemisphere of male Wistar rats was insonated with a 500 kHz transducer adapted to a stereotactic positioning system. The transducer was driven by a function/arbitrary waveform generator and amplifier. (**b**) To demonstrate successful opening of the BBB, rats underwent magnetic resonance imaging 30 minutes after insonation. Gadolinium-enhanced T1-weighted images showed a slight contrast enhancement in the focus of the insonation site (see arrow).

primates[21] will probably hinder the shift towards a human translation of intravascular AAV9 delivery. Moreover, the intravascular route of administration does not allow a focused vector delivery to predefined brain structures.

The aim of our study was to facilitate rAAV gene transfer into the CNS after noninvasive application. For this purpose, we combined intravenous (IV) administration of the chimeric rAAV2/1 with ultrasonographic localized opening of the BBB in adult rats. We found evidence that transient BBB disruption by ultrasound in the presence of microbubbles allows rAAV2/1 entry into the CNS with subsequent transduction of neuronal cells.

Results

Opening of the BBB

For BBB opening, one hemisphere of all rats was sonicated as shown in **Figure 1a**. To confirm a transient disruption of the BBB with the employed ultrasound parameters, two rats received a solution of UCA without viral vectors and underwent magnetic resonance imaging at 9.4 Tesla about 30 minutes after insonation of the left hemisphere.

In coronal sections, contrast-enhanced T1-weighted images after application of gadolinium showed a slight extravasation of the magnetic resonance imaging contrast agent in the left hemisphere as demonstrated in **Figure 1b**. The linear contrast enhancement was most prominent in the near-focus cortical area, but extended to the underlying striatum (see arrow). As gadolinium does not pass the intact BBB, these data substantiate the BBB opening.

β-galactosidase expression: histochemistry

To demonstrate a successful gene transfer, we analyzed the expression of LacZ 1 week after insonation in the presence of intravenously administered viral vectors. Histochemical analyses were performed to detect the distribution of β-galactosidase, the *LacZ* gene product, enzymatically.

A blue staining, produced by cleavage of X-gal by active β-galactosidase, was observed only in focal mostly cortical areas of the insonated left hemisphere (**Figure 2a,c,d**), whereas the complete contralateral, noninsonated hemisphere, was not stained (**Figure 2b**). Most β-gal–positive foci were located in close vicinity to blood vessels and

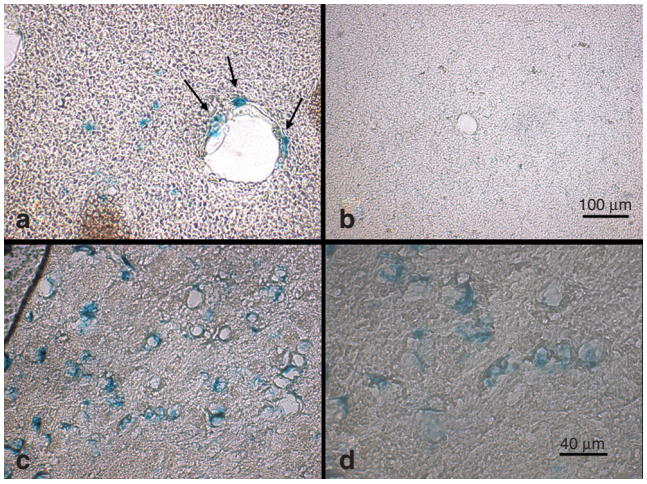

Figure 2 Histochemical demonstration of β-galactosidase in transfected cells. One week after insonation, histochemistry for detection of the enzymatic activity of the β-galactosidase protein was performed to demonstrate the correct processing of the protein product. The (**a**, **c**, **d**) resulting blue X-gal staining product could be detected in mostly cortically located spots of the insonated hemisphere, partially in close proximity to capillaries or in cells forming part of the vessel wall (**a**, see arrows). In contrast, (**b**) no β-galactosidase activity was observed in the noninsonated hemisphere. Magnifications were: **a**, **b**, ×50; **c**, ×200; **d**, ×400.

capillaries as depicted in **Figure 2a**. In addition to near-vascular β-galactosidase expressing cells in the brain parenchyma, we also found successfully transduced cells forming part of the vessel walls (see arrows). Higher magnification (**Figure 2c,d**) showed multiple spotted cells in the brain cortex with intracellular β-galactosidase.

Immunofluorescence microscopy

To further substantiate these results, we performed immunofluorescence (IF) microscopy with a monoclonal antibody against β-galactosidase from *E. coli*, allowing a differentiation between endogenous and transduced β-galactosidase. Taking advantage of the high sensitivity of IF staining, we could demonstrate a widespread expression of β-galactosidase in clusters of several hundred cells (**Figure 3a**). Most of these clusters encircled a central blood vessel as shown in

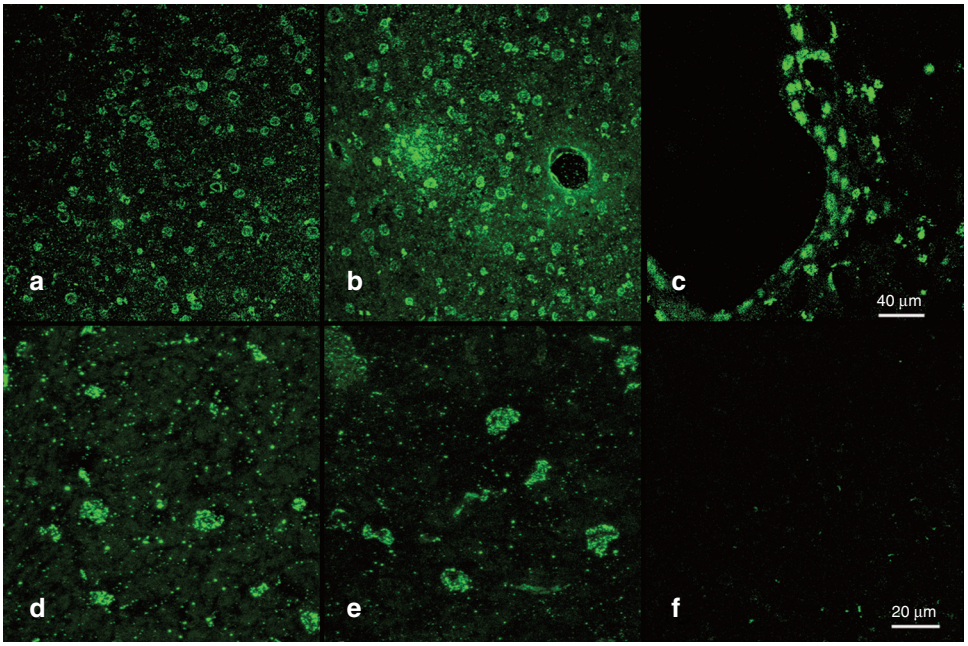

Figure 3 Immunofluorescence microscopy of β-galactosidase expression. To differentiate between endogenous and transduced β-galactosidase expression, immunofluorescence with antibodies specific against the bacterial β-galactosidase (coupled to Alexa-488, green) was performed. At lower magnification, (**a**–**c**) clusters of up to several hundred β-galactosidase expressing cells could be detected (magnification ×200), some of them centered around (**b**) capillaries or small vessels or (**c**) at the cortical surface. (**d**, **e**) At higher magnification (magnification ×630), a widespread punctuate staining pattern together with a more homogenous staining of the whole cytoplasm of transduced cells was observed. (**f**) The contralateral noninsonated hemisphere did not show any β-galactosidase expression.

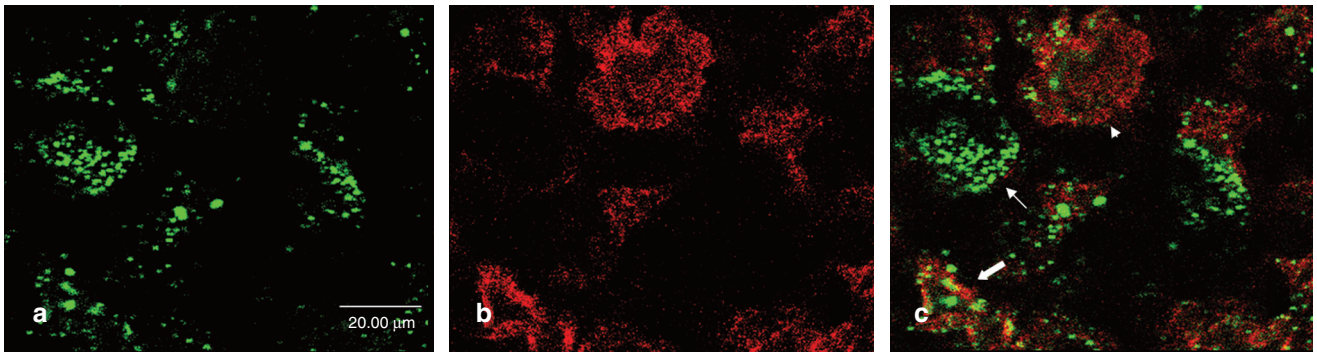

Figure 4 Double immunofluorescence with antibodies against tubulinIII. To specify the transduced cell types, (**a**) double immunolabeling with antibodies against β-galactosidase (coupled to Alexa-488, green) and (**b**) against the neuronal marker protein tubulinIII (coupled to Alexa-594, red) was performed. (**c**) Merge picture shows that almost all β-galactosidase expression occurs in cells staining positive for tubulinIII (see arrows), indicating that most of the transduced cells are neurons.

Figure 3b. Comparable to the histochemical results, most of the cells of the capillary wall also stained positive for bacterial β-galactosidase (Figure 3b). A high density of successfully transduced cell could further be located in proximity to the leptomeningeal cortical surface as demonstrated in Figure 3c. Overall, β-galactosidase positive reaction products were limited to a restricted mainly cortical area of the left hemisphere. At higher magnification, we noticed two different staining patterns in β-galactosidase expressing cells. A scattered and punctuate staining pattern was observed in a widespread area whereas some cells displayed a dense homogenous staining pattern excluding the nucleus (Figure 3d,e). Most β-gal–positive cells exhibited an oval-shaped morphology and differed only little in terms of size and shape.

The contralateral hemisphere showed no expression of bacterial β-galactosidase, indicating that successful gene transfer only occurred in the insonated hemisphere (Figure 3f).

To further characterize the transduced cell types, we performed double-IF microscopy with antibodies against β-galactosidase and cellular marker proteins. Double immunolabeling with antibodies against the neuronal marker tubulinIII showed that the vast majority of β-galactosidase expressing cells stained positive for tubulinIII as seen in the overlay in Figure 4c. DAPI (4′,6′-diamidino-2-phenylindole hydrochloride) staining of the neuronal nuclei confirmed the

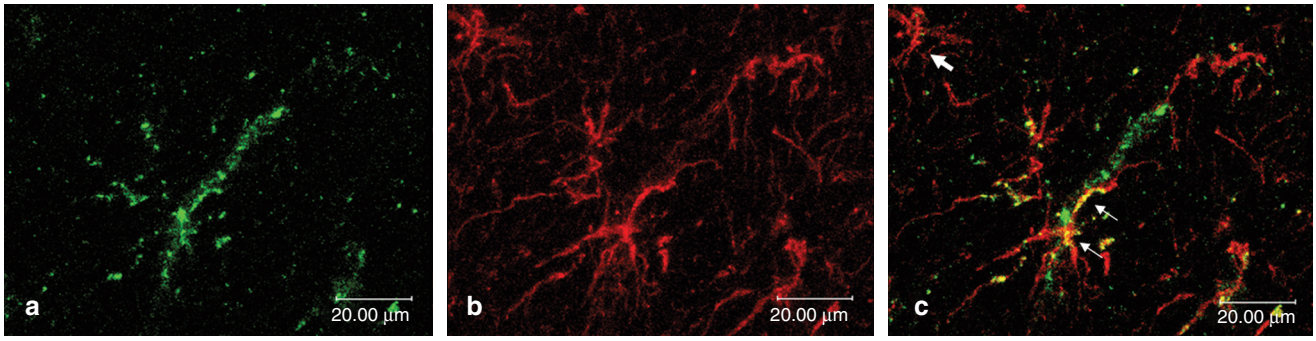

Figure 5 Double immunofluorescence with antibodies against GFAP. To evaluate the transduction of nonneuronal glial cells, (**a**) colocalization of β-galactosidase (coupled to Alexa-488, green) and (**b**) the astrocytic marker protein GFAP (coupled to Alexa-594, red) was investigated. (**c**) As shown in the merge picture, one GFAP-positive cell displays a β-galactosidase staining (see small arrows), whereas other astrocytes do not show a colocalization with β-galactosidase (see big arrow). These data demonstrate that a small fraction of transduced cells belong to the astrocytic cell line.

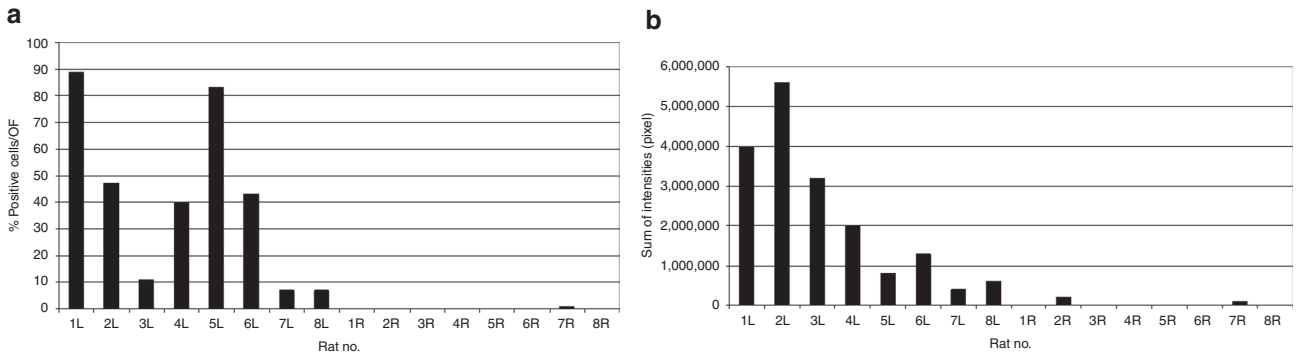

Figure 6 Quantification of β-galactosidase expression. (**a**) To evaluate the number of successfully transduced cells, all β-galactosidase expressing cells per optical field (OF) were counted. At least ten OFs per animal and hemisphere were considered (L, left hemisphere; R, right hemisphere). (**b**) Likewise, the sum of intensities defined as number of positive pixels per OF was quantified for both the insonated left hemisphere and the noninsonated right hemisphere. Values for control animals without administration of recombinant viral particles were omitted because we never found any positive reacting cells in these animals.

strictly cytoplasmic β-gal expression in neurons. These findings are in accordance with previous data on rAAV2/1 cell tropism,[19] showing that almost exclusively neurons were successfully transduced.

To demonstrate whether glial cells also were transduced by the recombinant particles, double immunoflorescence was performed using antibodies against the GFAP protein, known to be a specific astroglial marker protein. As shown in **Figure 5**, a small proportion of the GFAP-positive cells also stained for β-galactosidase, thus demonstrating that astrocytes were also transduced.

Quantification of transduction rate

As described above, IF microscopy was used to quantify expression rate in transduced cells. In a first set of experiments, the percentage of cells positive for β-gal expression was calculated. As shown in **Figure 6a**, the amount of positive cells varied between the different animals analyzed. In most of the cases, a large proportion up to 90% of the cells stained positive for β-galactosidase in the insonated hemisphere, whereas in three animals, the transduction rates were lower (1L–8L). No significant staining was observed in the contralateral hemisphere (1R–8R). In the control animals without injected viral particles, no staining at all was detected (data not shown). Corresponding to these results, quantification of the total staining intensity in the second set of experiments (**Figure 6b**) showed high sum intensities in the insonated hemispheres of the animals (1L–8L) whereas IV administration of recombinant viral particles without insonation did not lead to relevant intensity values (1R–8R). Thus, these results indicate that a large proportion of the cells can be targeted by the recombinants viruses, being most of them identified as neurons.

Discussion

Gene therapy is a promising new strategy for the treatment of various CNS diseases. However, the delivery of vector genomes to the brain is hampered by the intact BBB, separating the vascular compartment from the brain parenchyma. Our study now demonstrates that ultrasound-induced BBB opening in combination with IV AAV2/1 vectors (i) facilitates the entry of the viral vectors in the CNS, (ii) leads to an efficient and focal transduction in the sonicated regions, and (iii) targets mainly neuronal cells.

Recombinant adeno-associated viral vectors are counted among the most commonly used viral vector systems for gene delivery. AAV vectors offer several advantages compared with other vector systems including low immunogenicity and mediation of a high-level and long-term expression. With the characterization of different serotypes displaying different cell tropisms, a more specific transduction of cell types could be realized (for a review, see ref. 22). The limited transgene capacity of about 5 kb, often pointed out as a main disadvantage of AAV vector systems, has significantly been enhanced by usage of short promoters and transcriptional control elements.[23]

The flexibility of AAV-based vector systems has led to a broad interest in clinical applications. To date, several Phase I studies of degenerative CNS diseases have been completed or are still ongoing with promising results.[11,12] In patients with advanced Parkinson's disease, gene transfer of glutamic acid decarboxylase was successfully achieved by stereotactic injection of rAAV2-glutamic acid decarboxylase in the subthalamic nucleus.[11] However, the initial enthusiasm was trimmed back due to a high percentage of periprocedural complications of direct CNS injections.

To avoid invasive application methods, new strategies to overcome the BBB are needed. Recently, several studies have highlighted the ability of the AAV serotype 9 to cross the intact BBB, probably by active transport mechanisms. In rodents, intravascular delivery of rAAV9 led to a long-lasting transduction of neurons and glial cells throughout the whole brain.[20] However, in nonhuman primates, a shift in the cell tropism towards a predominant transduction of glial cells was observed.[21] Moreover, a translation into a clinical application is hindered by pre-existing neutralizing antibodies and a high peripheral tropism.[21] Even disregarding these limitations, it has to be considered that gene therapy with AAV9 will always lead to an overflow with AAV9 of the whole CNS: as this serotype will cross the BBB spontaneously after IV administration, the expression of the transgene cannot be limited to the region of interest. For the most CNS diseases like tumors, stroke or basal ganglia diseases like Parkinson's disease or Huntington's disease, a transduction of the whole CNS is neither necessary nor desirable. In these cases, a precisely localized gene delivery into the target region would be of utmost interest. In the last few years, focused ultrasound in the presence of gas-filled microbubbles has been shown to promote a focal and reversible BBB opening.[24] Depending on various sonication parameters like acoustic pressure or microbubble concentration, optimized protocols with avoidance of cell and tissue damage have been worked out.[6] Several preclinical animal studies using ultrasound-induced BBB opening have been conducted with a focus on neurooncology,[25] indicating effective delivery of chemotherapeutics. The exact entry mechanism into the CNS is yet under investigation, but experimental studies point at diffusion through the paracellular route following transient disintegration of tight junctions[26] and increased caveolae-mediated transport.[8]

In our experiments, histochemical detection of a blue staining, produced by cleavage of X-gal, proved the successful transduction of neuronal cells with expression of active β-galactosidase. Transduction of cells with AAV requires not only overcoming the BBB but also uptake of the viral particles via endocytosis with endosomal acidification, enhancing their phospholipase activity.[27] Our results therefore support previous hypotheses, suggesting that drug delivery into target cells by ultrasound in combination with microbubbles results mainly from enhanced endocytosis.[10,28] Consistent with this conclusion, we could demonstrate in a previous *in vitro* study that modification of rAAV particles by PEGylation impedes successful transduction, possibly by impaired interaction with cell membrane receptors needed for receptor mediated endocytosis.[29]

Quantification of the transduction rates showed a large amount of transgene expression strictly limited to the sonicated regions. The transduction efficiency is a major advantage in the usage of viral gene transfer compared with the naked plasmid DNA. Huang and colleagues[10] investigated the targeted delivery of the exogenous gene *pBDNF-EGFP* by focused ultrasound and microbubbles in 4-week-old mice. They found that enhanced green fluorescent protein expression was limited to the cytoplasm of only some neurons at the sonicated regions. Consequently, most clinical gene transfer studies have concentrated on viral vector strategies.

To specify the cell tropism of distinct rAAV serotypes, chimeric or pseudotyped vectors have recently been designed.[19] Genomes containing the terminal repeats of a commonly used serotype, mostly AAV2, can be packaged in capsids of another serotype, resulting in modifications of transduction distribution and efficiency. For our study, we constructed the chimeric rAAV2/1 which resulted in a widespread transduction of almost exclusively neurons in the sonicated regions. This observed pattern is consistent with previous studies, demonstrating that direct injection of rAAV2/1 in several brain structures of rats led to a higher number of transduced cells and a higher volume of distribution compared with the nonchimeric rAAV2/2.

By choosing an appropriate promoter, both the cell tropism and the transduction efficiency can further be increased. In our experiments, we used the strong cytomegalovirus (CMV) immediate-early promoter as vectors containing the CMV promoter have been shown to almost exclusively transduce neurons.[16] In addition, creation of hybrid form promoters[30] and insertion of transcriptional control elements[31] have recently led to optimized transduction efficiency.

To further target gene therapy vectors, cell type-specific binding ligands at the capsid surface have lately been investigated.[32] Mueller and colleagues were the first to design random AAV peptide libraries in which each virus particle exhibits a random peptide at the capsid surface. By this means, specific AAV vectors targeting endothelial cells[33] as well as other cell lines or tissues have been selected.

Concluding, we could demonstrate for the first time the feasibility of a localized AAV gene transfer into the CNS by ultrasound-induced BBB opening. The numerous redevelopments in vector engineering allow for very specific modeling of viral vectors, thus providing an encouraging new treatment strategy for CNS diseases.

Materials and methods

Vectors. The engineering of AAV vectors was conducted as described elsewhere.[34] Briefly, vector production was

effected by cotransfection of vector plasmid pUF3nlsLacz[35] and helper plasmid pDP1[36] in 293T cells. The vector plasmid encodes for AAV2 terminal repeat elements and the transgene *nlsLAcZ* (nuclear localization signal; β-galactosidase) driven by a CMV promoter. The helper plasmid enclosed an AAV1 cap. The titers of the vector preparation were 5.3×10^{11} encapsidated vector genomes/ml.

Ultrasound device. For BBB opening, a 500 kHz transducer (H-104MR) was driven by a function generator (Agilent 33120 A Function/Arbitrary Waveform Generator; Agilent Technologies, Santa Clara, CA) and amplifier (model 40AD1; AR Amplifier Research, Souderton, PA). The transducer was adjusted to a cone filled with deionized water and adapted to a stereotactic positioning system (**Figure 1a**). The distal cone aperture with a diameter of 5 mm was stereotactically concentrated on the left hemisphere, the contralateral hemisphere was used as intraindividual control. The basic principles of focused ultrasound are described in **Supplementary Figure S1**. The pressure amplitude was 2.2 MPa as measured by a calibrated 400 µm diameter hydrophone (HGL 400; Onda, Sunnyvale, CA). Assuming a total pressure lost of 49% due to attenuation through the rat skull as described previously,[9] the effective pressure amplitude was estimated at about 1.1 MPa. The burst count was 10 ms at a repetition frequency of 1 Hz.

Vascular acoustic resonators. The vascular acoustic resonators (BR38) were kindly provided by Bracco Research, Plan-Les-Ouates. BR38 are gas-filled (fluorocarbon—air) vascular acoustic resonators with a lipidic shell, a number mean diameter of 1.4 µm and a volume mean diameter of 3.6 µm. The concentration for a dispersion in saline was 0.2×10^9 bubbles/ml.

Animal model. All animals were approved by the local government authorities in accordance with the animal protection guidelines. Fourteen male Wistar rats (Charles River, Sulzfeld, Germany) weighing 465 ± 48 g were anesthetized with 1.5% isofluorane, body temperature was controlled with a heating pad. The hair over the skull was removed with depilatory cream, and the tail vein was catheterized. All rats underwent insonation of the left hemisphere over 40 seconds. Simultaneously, eight of these received 1.06×10^{11} encapsidated vector genomes dispersed in a solution of UCA (BR38; Bracco Research, Princeton, NJ) at a concentration of 0.1 ml/kg body weight via the tail vein catheter. Four further animals were insonated as described above, together with IV administration of UCA, but without administration of recombinant viral particles. Finally, two more rats received a solution of UCA without viral vectors instead and were used for approval of BBB opening by magnetic resonance imaging (9.4 Tesla Bruker BioSpec 94/20 USR; Tesla, Karlsruhe, Germany).

All animals were killed after 7 days by transcardial perfusion with 2% paraformaldehyde and 0.5% glutaraldehyde in deep anesthesia. Brains were removed and incubated in 2% paraformaldehyde and 0.5% glutaraldehyde at 4 °C overnight, followed by incubation in sucrose 30% at 4 °C for 3 hours. After freezing in ice-cold isopentan, the brains were stored at –80 °C until processing.

Immunohistochemistry. Coronal sections were cut at 10 µm on a freezing microtome (Leica CM 1900; Leica, Bensheim, Germany) and treated with 10 mmol/l TRIS–HCl at 98 °C for demasking. For detection of β-galactosidase, we used a β-Gal Staining Kit Cat. No. K1465-01, Invitrogen (Carlsbad, CA). Sections were rinsed in phosphate-buffered saline 1× and afterwards incubated in fixation solution for 10 minutes. After two washing steps in phosphate-buffered saline 1×, the sections were incubated for 48 hours in staining solution containing 5-bromo-4-chloro-3-indolyl-β-D-galactopyranoside (X-Gal) at 37 °C in a humidified incubator.

Immunofluorescence. Cryosections of 10 µm were treated with TBS-Triton 0.2% and afterwards incubated with a monoclonal antibody against β-galactosidase from *E. coli* (SM3002P; Acris Antibodies, Herford, Germany) overnight at 37 °C. Sections were then washed in TBS-Triton 0.2% and afterwards incubated with a goat antimouse antibody coupled to Alexa Fluor 488 (1:800; Invitrogen). After washing in TBS-Triton 0.2%, sections were mounted in antifading medium. Pictures were taken with a confocal microscope (Leica DM IRBE; Leica and Olympus FluoView FV1000; Olympus, Tokyo, Japan).

For double immunolabeling with antibodies against cellular marker proteins, the following primary and secondary antibodies were used: α-β-Gal (monoclonal mouse, SM3002P; Acris), α-tubulinIII (polyclonal rabbit, ab18207; Abcam), α-GFAP (polyclonal rabbit, ab7260; Abcam), goat antimouse-Alexa 488 (1:800; Invitrogen), goat antirabbit-Alexa 594 (1:800; Invitrogen) and DAPI 100 ng/ml working solution.

Quantification of transduction rates. For quantification of transduction rates, the expression of β-galactosidase was analyzed using IF microscopy. Two different parameters were considered: the number of cells expressing β-galactosidase, irrespective of the intensity of such expression, and the total intensity per optical field of the β-galactosidase expression, irrespective of the number of cells transduced. Thus, number of transfected cells and intensity of expression were quantified independently. For this, serial sections of the brain were prepared and every second slice was viewed under the microscope. Using a computer program, the section with the largest amount of pixels (taken as a measure of expression intensity) was identified. Pictures were taken from integrated images of this slice and analyzed as described.[37] For quantification, two control groups were used: to evaluate the effect of IV administered recombinant viral particles without ultrasound-induced BBB opening, the contralateral hemispheres of the eight insonated rats were always examined. A second control group were animals treated with ultrasound and microbubbles but without injection of viral recombinant particles. Quantification was performed in a double-blinded form.

Supplementary material

Figure S1. Schematic drawing demonstrating the principle of focused ultrasound-gene delivery.

Acknowledgments. The research leading to these results has received funding from the European Union's Seventh

Framework Programme (FP7/2007–2013) under grant agreements n° 201024 and n° 202213 (European Stroke Network)". We kindly thank Bracco Research for providing the novel vascular acoustic resonators BR38. The authors declare no competing financial interest.

1. Meairs, S and Alonso, A (2007). Ultrasound, microbubbles and the blood-brain barrier. *Prog Biophys Mol Biol* **93**: 354–362.
2. Pardridge, WM (2005). The blood-brain barrier: bottleneck in brain drug development. *NeuroRx* **2**: 3–14.
3. Alonso, A, Reinz, E, Fatar, M, Jenne, J, Hennerici, MG and Meairs, S (2010). Neurons but not glial cells overexpress ubiquitin in the rat brain following focused ultrasound-induced opening of the blood-brain barrier. *Neuroscience* **169**: 116–124.
4. Alonso, A, Reinz, E, Fatar, M, Hennerici, MG and Meairs, S (2011). Clearance of albumin following ultrasound-induced blood-brain barrier opening is mediated by glial but not neuronal cells. *Brain Res* **1411**: 9–16.
5. Hynynen, K, McDannold, N, Vykhodtseva, N and Jolesz, FA (2001). Noninvasive MR imaging-guided focal opening of the blood-brain barrier in rabbits. *Radiology* **220**: 640–646.
6. Samiotaki, G, Vlachos, F, Tung, YS and Konofagou, EE (2012). A quantitative pressure and microbubble-size dependence study of focused ultrasound-induced blood-brain barrier opening reversibility *in vivo* using MRI. *Magn Reson Med* **67**: 769–777.
7. Sheikov, N, McDannold, N, Sharma, S and Hynynen, K (2008). Effect of focused ultrasound applied with an ultrasound contrast agent on the tight junctional integrity of the brain microvascular endothelium. *Ultrasound Med Biol* **34**: 1093–1104.
8. Deng, J, Huang, Q, Wang, F, Liu, Y, Wang, Z, Wang, Z *et al.* (2012). The role of caveolin-1 in blood-brain barrier disruption induced by focused ultrasound combined with microbubbles. *J Mol Neurosci* **46**: 677–687.
9. Treat, LH, McDannold, N, Vykhodtseva, N, Zhang, Y, Tam, K and Hynynen, K (2007). Targeted delivery of doxorubicin to the rat brain at therapeutic levels using MRI-guided focused ultrasound. *Int J Cancer* **121**: 901–907.
10. Huang, Q, Deng, J, Wang, F, Chen, S, Liu, Y, Wang, Z *et al.* (2012). Targeted gene delivery to the mouse brain by MRI-guided focused ultrasound-induced blood-brain barrier disruption. *Exp Neurol* **233**: 350–356.
11. LeWitt, PA, Rezai, AR, Leehey, MA, Ojemann, SG, Flaherty, AW, Eskandar, EN *et al.* (2011). AAV2-GAD gene therapy for advanced Parkinson's disease: a double-blind, sham-surgery controlled, randomised trial. *Lancet Neurol* **10**: 309–319.
12. Mandel, RJ (2010). CERE-110, an adeno-associated virus-based gene delivery vector expressing human nerve growth factor for the treatment of Alzheimer's disease. *Curr Opin Mol Ther* **12**: 240–247.
13. McCown, TJ (2011). Adeno-Associated Virus (AAV) Vectors in the CNS. *Curr Gene Ther* **11**: 181–188.
14. Tenenbaum, L, Chtarto, A, Lehtonen, E, Velu, T, Brotchi, J and Levivier, M (2004). Recombinant AAV-mediated gene delivery to the central nervous system. *J Gene Med* **6 Suppl 1**: S212–S222.
15. Mastakov, MY, Baer, K, Symes, CW, Leichtlein, CB, Kotin, RM and During, MJ (2002). Immunological aspects of recombinant adeno-associated virus delivery to the mammalian brain. *J Virol* **76**: 8446–8454.
16. McCown, TJ, Xiao, X, Li, J, Breese, GR and Samulski, RJ (1996). Differential and persistent expression patterns of CNS gene transfer by an adeno-associated virus (AAV) vector. *Brain Res* **713**: 99–107.
17. Davidson, BL, Stein, CS, Heth, JA, Martins, I, Kotin, RM, Derksen, TA *et al.* (2000). Recombinant adeno-associated virus type 2, 4, and 5 vectors: transduction of variant cell types and regions in the mammalian central nervous system. *Proc Natl Acad Sci USA* **97**: 3428–3432.
18. Chao, H, Liu, Y, Rabinowitz, J, Li, C, Samulski, RJ and Walsh, CE (2000). Several log increase in therapeutic transgene delivery by distinct adeno-associated viral serotype vectors. *Mol Ther* **2**: 619–623.
19. Burger, C, Gorbatyuk, OS, Velardo, MJ, Peden, CS, Williams, P, Zolotukhin, S *et al.* (2004). Recombinant AAV viral vectors pseudotyped with viral capsids from serotypes 1, 2, and 5 display differential efficiency and cell tropism after delivery to different regions of the central nervous system. *Mol Ther* **10**: 302–317.
20. Foust, KD, Nurre, E, Montgomery, CL, Hernandez, A, Chan, CM and Kaspar, BK (2009). Intravascular AAV9 preferentially targets neonatal neurons and adult astrocytes. *Nat Biotechnol* **27**: 59–65.
21. Gray, SJ, Matagne, V, Bachaboina, L, Yadav, S, Ojeda, SR and Samulski, RJ (2011). Preclinical differences of intravascular AAV9 delivery to neurons and glia: a comparative study of adult mice and nonhuman primates. *Mol Ther* **19**: 1058–1069.
22. Vasileva, A and Jessberger, R (2005). Precise hit: adeno-associated virus in gene targeting. *Nat Rev Microbiol* **3**: 837–847.
23. Kügler, S, Lingor, P, Schöll, U, Zolotukhin, S and Bähr, M (2003). Differential transgene expression in brain cells *in vivo* and *in vitro* from AAV-2 vectors with small transcriptional control units. *Virology* **311**: 89–95.
24. Konofagou, EE, Tung, YS, Choi, J, Deffieux, T, Baseri, B and Vlachos, F (2012). Ultrasound-induced blood-brain barrier opening. *Curr Pharm Biotechnol* **13**: 1332–1345.
25. Liu, HL, Yang, HW, Hua, MY and Wei, KC (2012). Enhanced therapeutic agent delivery through magnetic resonance imaging-monitored focused ultrasound blood-brain barrier disruption for brain tumor treatment: an overview of the current preclinical status. *Neurosurg Focus* **32**: E4.
26. McDannold, N, Vykhodtseva, N, Raymond, S, Jolesz, FA and Hynynen, K (2005). MRI-guided targeted blood-brain barrier disruption with focused ultrasound: histological findings in rabbits. *Ultrasound Med Biol* **31**: 1527–1537.
27. Bartlett, JS, Wilcher, R and Samulski, RJ (2000). Infectious entry pathway of adeno-associated virus and adeno-associated virus vectors. *J Virol* **74**: 2777–2785.
28. Meijering, BD, Juffermans, LJ, van Wamel, A, Henning, RH, Zuhorn, IS, Emmer, M *et al.* (2009). Ultrasound and microbubble-targeted delivery of macromolecules is regulated by induction of endocytosis and pore formation. *Circ Res* **104**: 679–687.
29. Geers, B, Lentacker, I, Alonso, A, Sanders, NN, Demeester, J, Meairs, S *et al.* (2011). Elucidating the mechanisms behind sonoporation with adeno-associated virus-loaded microbubbles. *Mol Pharm* **8**: 2244–2251.
30. Gray, SJ, Foti, SB, Schwartz, JW, Bachaboina, L, Taylor-Blake, B, Coleman, J *et al.* (2011). Optimizing promoters for recombinant adeno-associated virus-mediated gene expression in the peripheral and central nervous system using self-complementary vectors. *Hum Gene Ther* **22**: 1143–1153.
31. Paterna, JC, Moccetti, T, Mura, A, Feldon, J and Büeler, H (2000). Influence of promoter and WHV post-transcriptional regulatory element on AAV-mediated transgene expression in the rat brain. *Gene Ther* **7**: 1304–1311.
32. Müller, OJ, Kaul, F, Weitzman, MD, Pasqualini, R, Arap, W, Kleinschmidt, JA *et al.* (2003). Random peptide libraries displayed on adeno-associated virus to select for targeted gene therapy vectors. *Nat Biotechnol* **21**: 1040–1046.
33. Varadi, K, Michelfelder, S, Korff, T, Hecker, M, Trepel, M, Katus, HA *et al.* (2012). Novel random peptide libraries displayed on AAV serotype 9 for selection of endothelial cell-directed gene transfer vectors. *Gene Ther* **19**: 800–809.
34. Grimm, D (2002). Production methods for gene transfer vectors based on adeno-associated virus serotypes. *Methods* **28**: 146–157.
35. Zolotukhin, S, Potter, M, Hauswirth, WW, Guy, J and Muzyczka, N (1996). A "humanized" green fluorescent protein cDNA adapted for high-level expression in mammalian cells. *J Virol* **70**: 4646–4654.
36. Grimm, D, Kay, MA and Kleinschmidt, JA (2003). Helper virus-free, optically controllable, and two-plasmid-based production of adeno-associated virus vectors of serotypes 1 to 6. *Mol Ther* **7**: 839–850.
37. Alonso, A, Reinz, E, Jenne, JW, Fatar, M, Schmidt-Glenewinkel, H, Hennerici, MG *et al.* (2010). Reorganization of gap junctions after focused ultrasound blood-brain barrier opening in the rat brain. *J Cereb Blood Flow Metab* **30**: 1394–1402.

Supplementary Information accompanies this paper on the Molecular Therapy–Nucleic Acids website (http://www.nature.com/mtna)